Electronic Supplementary Information for:

Synthesis of $CuInS_2$ nanocrystals from a molecular complex − characterization of the orthorhombic domain structure

Jorge L. Cholula-Díaz,[a] **Gerald Wagner,**[b] **Dirk Friedrich,**[a]
Oliver Oeckler,[b] **and Harald Krautscheid**∗[a]

[a] Institut für Anorganische Chemie, Universität Leipzig,
Johannisallee 29, 04103 Leipzig, Germany.
Fax: +49 (0)341-9736199; Tel: +49 (0)341-9736172;
E-mail: krautscheid@rz.uni-leipzig.de

[b] Institut für Mineralogie, Kristallographie und
Materialwissenschaft, Universität Leipzig, Scharnhorststrasse 20,
04275 Leipzig, Germany.

∗ To whom correspondence should be addressed

1 Synthesis of $[(Me_3P)_3Cu(SC_2H_4S)In^iPr_2]$ (1)

A solution of $[(Me_3P)_3Cu(SC_2H_4S)Cu(PMe_3)_3]$ is produced by stirring $(CuSC_2H_4S)_n$, prepared from Cu_2O and 1,2-ethanedithiol, together with PMe_3 in toluene. To 10 mL of the clear yellow solution containing 1.0 mmol of the complex 2.0 mmol of $In^iPr_3 \cdot 0.5\ Et_2O$ and 1 mmol of HSC_2H_4SH, diluted with toluene, are added. The initially yellow solution starts to evolve gas and fades until a colorless solution is obtained. After layering with 10 mL of n-heptane and storage at -20 °C for one day a colorless oil separates from which **1** crystallizes at -20 °C. The crystals are washed with n-pentane and dried in vacuo. Yield: 0.85 g (73 %). ^{1}H-NMR (C_6D_6, 400 MHz) δ_H in ppm: 3.08 (4H, s, ethylene), 1.85 (12H, d, br, $^3J_{HH}$ = 7.5 Hz, $InCH(CH_3)_2$), 1.55 (2H, septet, $^3J_{HH}$ = 7.5 Hz, $InCH(CH_3)_2$), 0.84 (27H, d, $^2J_{PH}$ = 3.6 Hz, PMe_3). $^{31}P\{^1H\}$-NMR (C_6D_6, 161.9 MHz) δ_P in ppm: -46.6. Elemental analysis found (calculated): C % 35.11 (34.91), H % 7.84 (7.75).

2 Simultaneous thermal analysis of 1

Simultaneous thermal analysis (STA) was performed using a ”STA 449 F1 Jupiter” Thermogravimetry (TG)/Differential Thermoanalysis (DTA) device (Netzsch) coupled with a ”Tensor 27” Fourier Transformation Infrared (FTIR) spectrometer (Bruker) and a ”QMS 403 C” electron ionization quadrupole mass spectrometer (Aëolos). The samples were transferred into Al_2O_3 crucibles within a drybox under nitrogen atmosphere. The samples were then transported to the STA device in a dry vessel in order to minimize contact with air. The oven was evacuated and flooded with helium carrier gas before measurements were started. The samples were heated from 10 to 600 °C with a rate of 10 K/min. DTA reference was an empty Al_2O_3 crucible.

Fig. S1 depicts the results of the STA of **1** under helium atmosphere. The onset of thermolysis is found at 101 °C. The toal mass loss adds up to 59.4 % and the process is fully completed at 440 °C. However, the main part of the mass loss is completed at 292 °C. The TG graph indicates a multi-step mechanism, which cannot clearly be resolved. The Gram-Schmidt graph shows five main peaks at 119 °C, 178 °C, 200 °C, 263 °C and 283 °C. An extraction of the corresponding gas phase Infrared (IR)-spectra measured by TG-IR coupling is shown in Fig. S2. A comparison with reference spectra reveals, that the first three peaks can be attributed to the evolution of gaseous PMe_3. At 263 °C a mixture of propane and ethylene gas is detected. And the last peak at 283 °C corresponds mainly to propane gas. Although propane gas is clearly detected by TG-IR coupling, it is reasonable to assume radical based thermolysis of isopropyl groups. The alkane is probably formed upon transfer through the 1.5 m long transfer hose that connects the oven unit of the TG apparatus with the gas flow IR cell. The actual total mass loss of 59.4 % is slightly higher than 58.5 % that are calculated for the formation of $CuInS_2$. This is explained by side reactions that take place during thermolysis.

Fig. S3 depicts the results of a Rietveld refinement performed on X-ray powder diffraction data of the TG residue of **1** after heating up to 900 °C. The main phase is

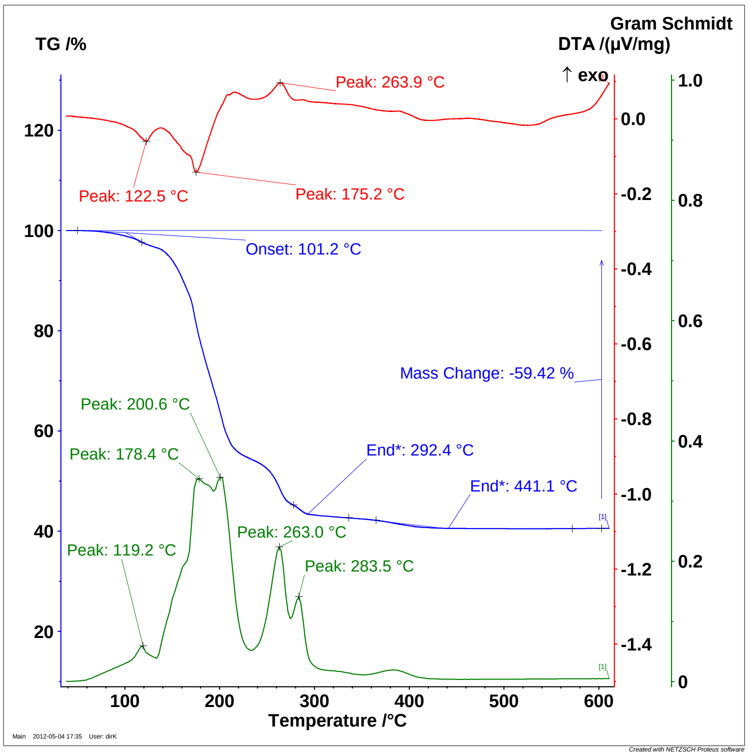

Figure S1: Simultaneous thermal analysis of $[(Me_3P)_3Cu(SC_2H_4S)In^iPr_2]$ (**1**).

chalcopyrite type $CuInS_2$, however, two minor phases can be detected: Small amounts of In_2O_3 and a copper indium alloy are formed by partial reductive elimination of In^iPr groups and partial reaction with traces of air and moisture after the TG experiment.

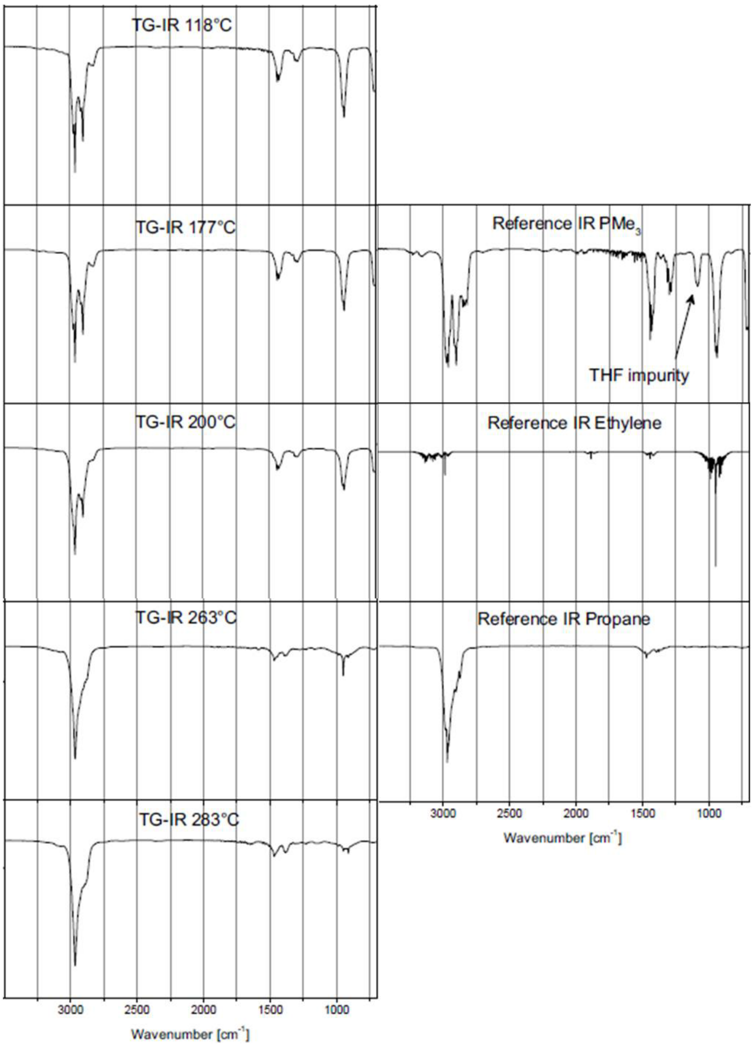

Figure S2: TG-IR spectra of $[(Me_3P)_3Cu(SC_2H_4S)In^iPr_2]$ (**1**) and reference spectra of PMe_3, C_2H_4 and C_3H_8 (NIST).

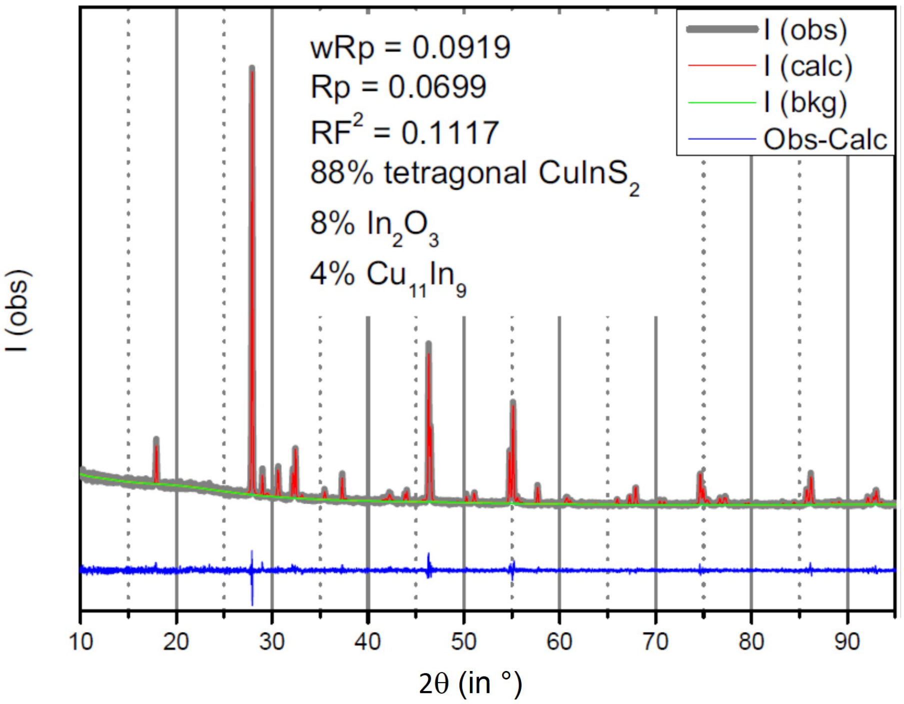

Figure S3: Rietveld refinement of the X-ray powder diffraction pattern of the TG residue of $[(Me_3P)_3Cu(SC_2H_4S)In^iPr_2]$ (**1**). Obs: observed; calc: calculated; bkg: background.

3 Crystallographic data of the hypothetical orthorhombic $CuInS_2$ modifications with space groups $Pmn2_1$ and $Pmc2_1$

Table S1: Crystal Data

Formula:	$CuInS_2$
Crystal System:	Orthorhombic
Space group:	$Pmn2_1$ or $Pmc2_1$
Lattice parameters§:	$a = 3.907$ Å, $b = 6.767$ Å, $c = 6.429$ Å

§ Derived from unit cell dimensions for hexagonal wurtzite $CuInS_2$.[S1]

Table S2: Atomic coordinates for orthorhombic $CuInS_2$ with space group $Pmn2_1$

Atom	Wyck.	x/a	y/b	z/c
In	a	0	7/12	0
Cu	a	0	11/12	1/2
S	a	0	7/12	3/8
S	a	0	11/12	7/8

Table S3: Atomic coordinates for orthorhombic $CuInS_2$ with space group $Pmc2_1$

Atom	Wyck.	x/a	y/b	z/c
In	a	0	1/3	0
Cu	b	1/2	5/6	0
S	a	0	2/3	7/8
S	b	1/2	1/6	7/8

4 Temperature-dependent powder XRD

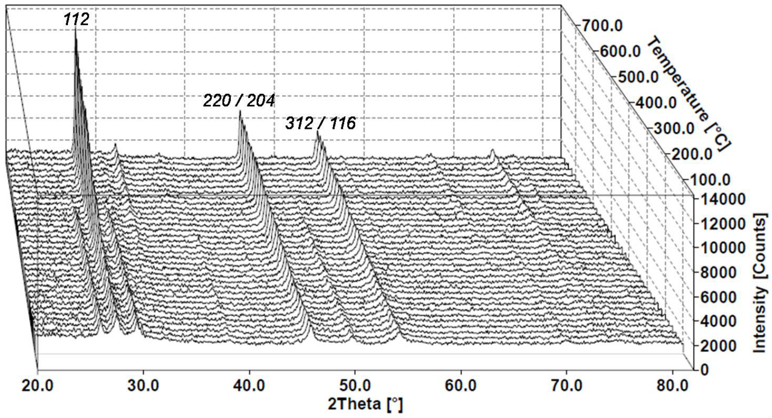

Figure S4: Temperature-dependent powder XRD pattern of $CuInS_2$ nanocrystals synthesized by thermolysis of $[(Me_3P)_3Cu(SC_2H_4S)In^iPr_2]$ ($\underline{\mathbf{1}}$) in 5 mL of dioctyl phthalate at $\sim$ 300 °C with 271 μL of oleylamine. The Miller indices correspond to chalcopyrite type $CuInS_2$.

5 TEM and HRTEM images, SAED patterns and EDX spectra

5.1 TEM images and EDX spectra

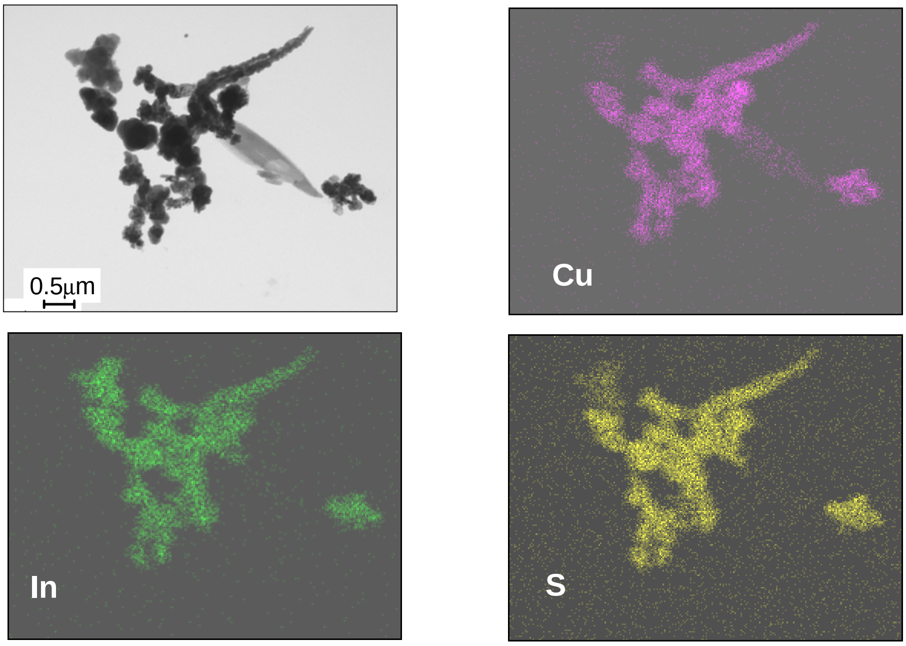

Figure S5: STEM bright-field image and spatial distribution of elements (EDX mapping) of the NP-CIS sample deposited by drop coating on a carbon-coated molybdenum TEM grid.

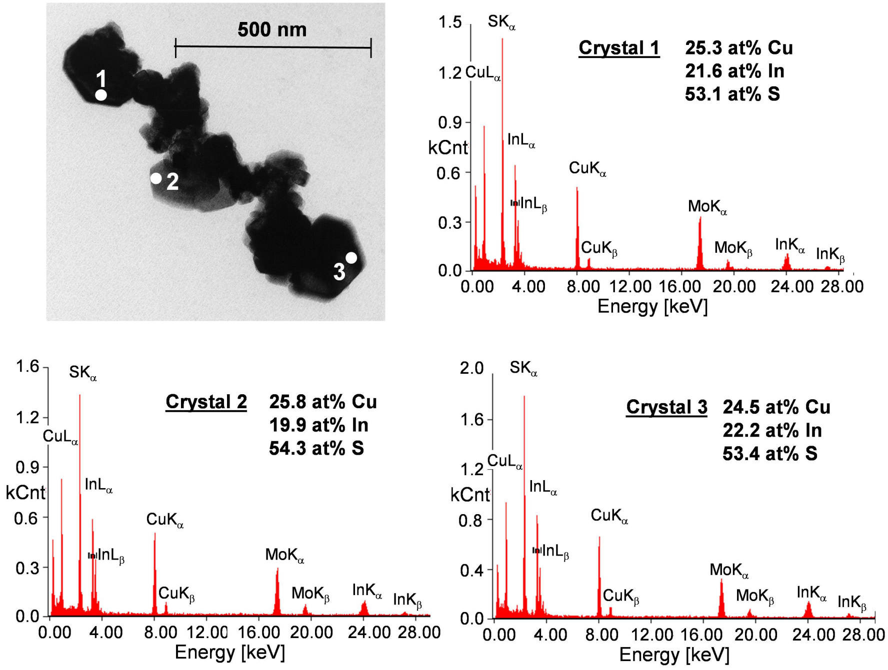

Figure S6: TEM image and EDX spectra of hexagonal-shaped $CuInS_2$ nanocrystals in the NP-CIS sample.

5.2 HRTEM images and SAED patterns

For HRTEM images and SAED patterns (Fig. S7), the $CuInS_2$ powder was mixed with M-Bond 610 glue. This mixture was fixed between two 400 μm thick GaAs wafers acting as inert material. From this package some slices of 3 mm length and about 600 μm thickness were cut by a wire saw. In addition, part of the material was mixed with Gatan M1 epoxy resin (fill material). The mixture was filled into a glass capillary (outer diameter 3 mm, inner diameter ca. 0.6 mm). After hardening of the epoxy resin, ca. 300 μm thick slices were cut as mentioned above. The GaAs as well as glass slices (cross section technique) were mechanically thinned by grinding (40 μm, 15 μm, 5 μm) and polished using a GATAN dimple grinder. To obtain electron transparency, the so-prepared samples were thinned by Ar^+ ions. Typical operation conditions employed during the first double-side ion milling are an accelerating voltage of 4 kV, beam currents of 0.5 mA and a beam incidence angle of 15°. Finally, an accelerating voltage of 2 kV for 20 min keeping unchanged the other parameters were employed for the second double-side ion milling.

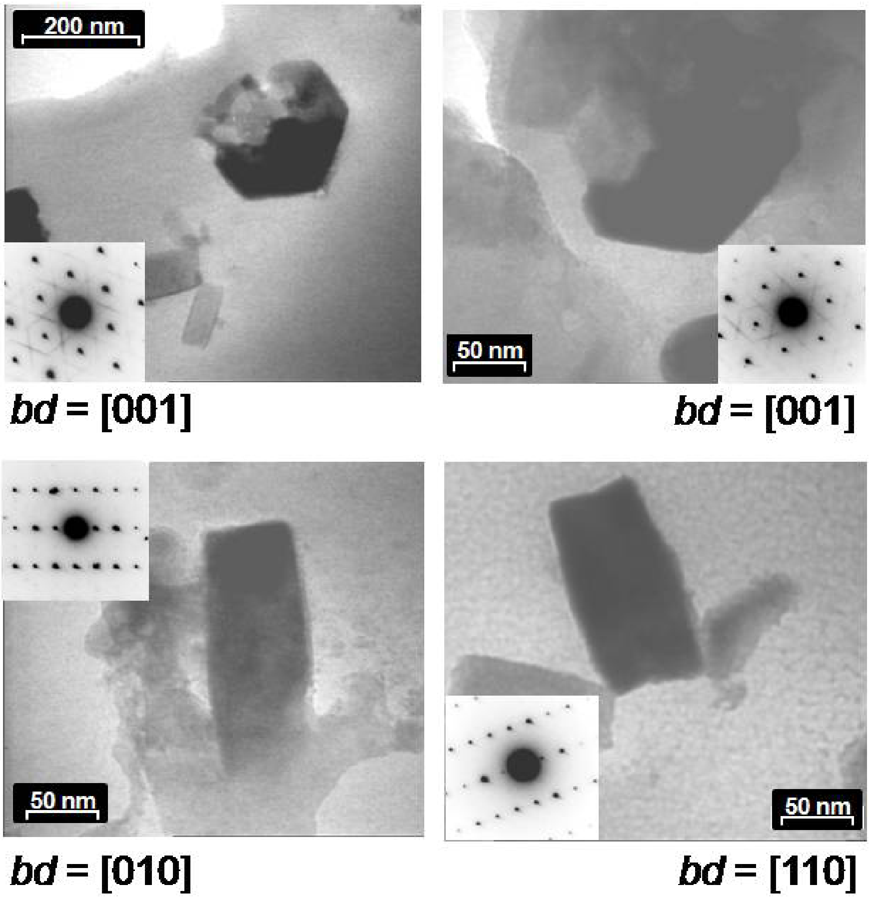

bd = [001]

bd = [001]

bd = [010]

bd = [110]

Figure S7: Morphology of $CuInS_2$ nanocrystals (found in the NP-CIS sample) used for electron diffraction and HRTEM imaging together with the corresponding SAED patterns.

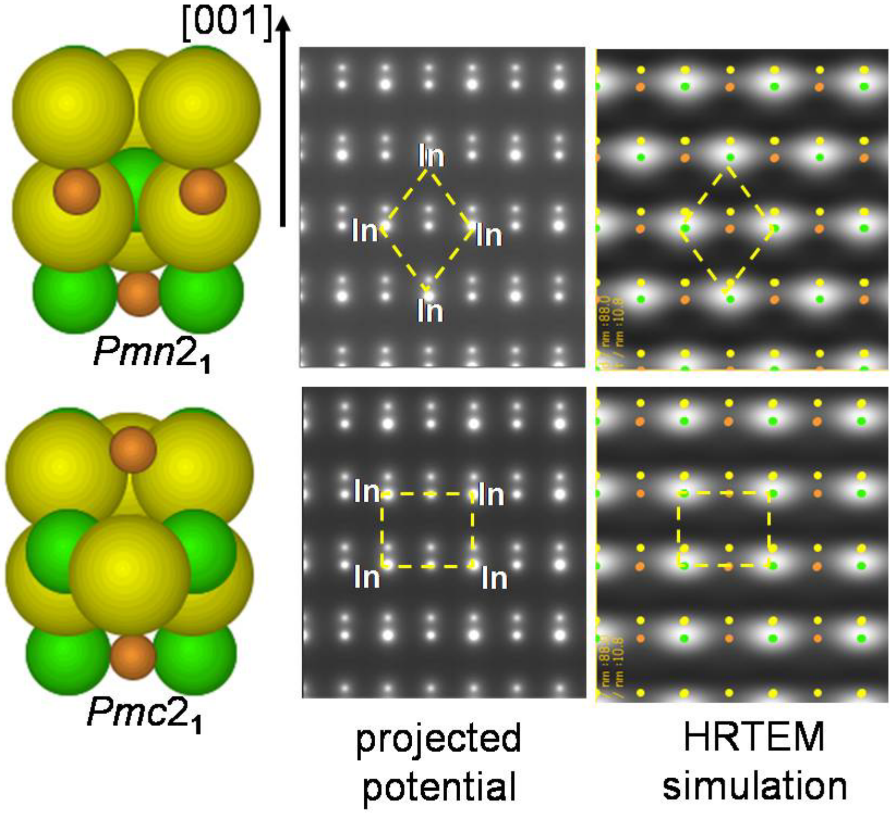

Figure S8: The correlation of HRTEM contrasts with atom positions is visualized for a better understanding of the different features in the simulated HRTEM patterns along zone axis $[010]_o$. Under the given imaging conditions, *i.e.* a thickness of 11 nm and an underfocus value of 88 nm ($\Delta f = -88$ nm; concerning the other values used for calculation see Fig. 8). The bright contrasts indicate the positions of indium atoms (green). Therefore, the relative positions of the indium atoms in $Pmn2_1$ yield a parallelogram, whereas in $Pmc2_1$ a rectangular arrangement is present (see dashed lines).

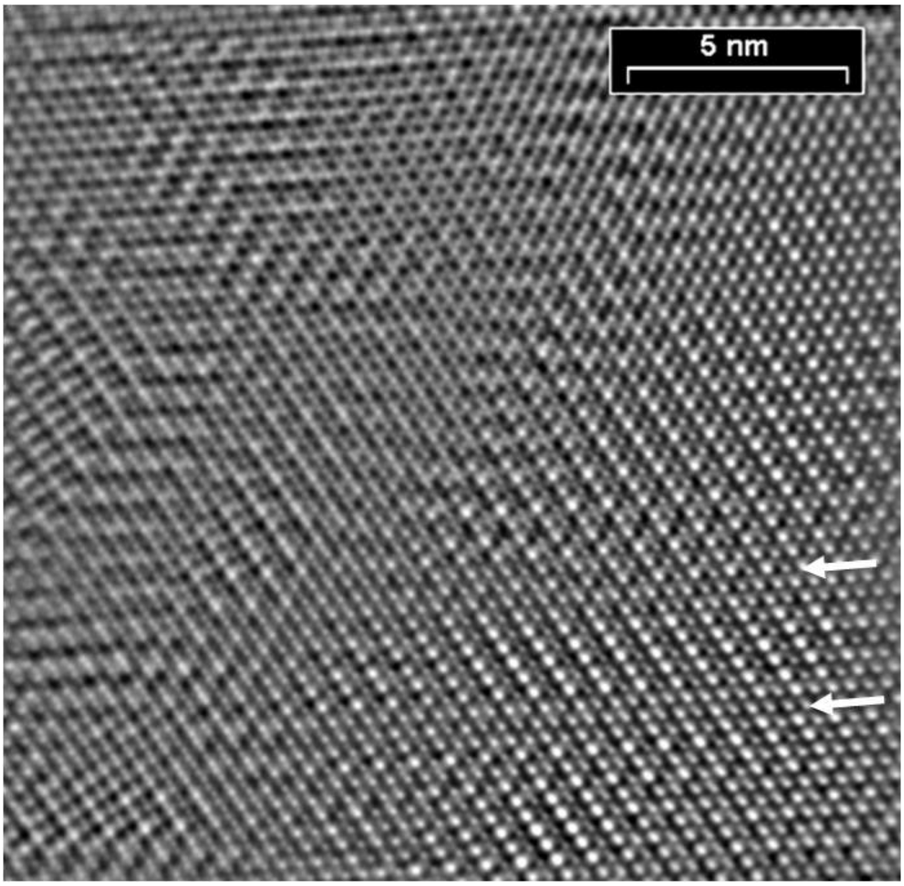

Figure S9: Experimental HRTEM image of a $CuInS_2$ nanocrystal (found in the NP-CIS sample). Zone axis $[001]_h$, $\Delta f = -54$ nm; Fourier filtered using the maxima at the wurtzite type's lattice nodes, 000 not included; the arrows mark two well-pronounced antiphase boundaries, which are not sharp because they lie inclined in the thin TEM specimen.

References

[S1] Y. Qi, Q. Li, K. Tang, Z. Liang, Z. Rhen, and X. Liu, *J. Phys. Chem. C*, 2009, **113**, 3939-3944.